# Unit 19
# Measurements of strain, stress, and coil mechanical properties

**Soren Prestemon and Steve Gourlay**
Lawrence Berkeley National Laboratory (LBNL)

With many thanks to **Paolo Ferracin**
CERN

# Outline

- Introduction
- Stress-strain measurements devices
  - Capacitive gauges
  - Strain gauges
- Measurements of coil properties
  - Elastic modulus
  - Thermal contraction
- Measurements of $Nb_3Sn$ wires and cables before and after heat treatment
- Some comments on modeling of material properties

# References


[1] N. Siegel, et al., "*Design and use of capacitive force transducers for superconducting magnet models for the LHC*", LHC Project Report 173.

[2] C.L. Goodzeit, et al., "*Measurement of internal forces in superconducting accelerator magnets with strain gauge transducers*", IEEE Trans. Magn., Vol. 25, No. 2, March 1989, p. 1463- 1468.

[3] M. Reytier, et al., "*Characterization of the thermo-mechanical behavior of insulated cable stacks representative of accelerator magnet coils*", IEEE Trans. Supercond., Vol. 11, Issue 1, March 2001, p. 3066 – 3069.

[4] K.P. Chow and G.A. Millos, "*Measurements of Modulus of Elasticity and Thermal Contraction of Epoxy Impregnated Niobium-Tin and Niobium-Titanium Composites*", IEEE Trans. Supercond., Vol. 9, Issue 2, June 1999, p. 213 – 215.

[5] D.R. Chichili, et al., "*Investigation of cable insulation and thermo-mechanical properties of epoxy impregnated $Nb_3Sn$ composites*", IEEE Trans. Supercond., Vol. 10, Issue 1, March 2000, p. 1317 – 1320.

# 1. Introduction

- The knowledge of the stress conditions in a superconducting magnet is mandatory
  - risk of excessive conductor motion in case of low pre-stress conditions
  - risk of conductor degradation or plastic deformation of the structure in case of high stresses.

- In order to predict the mechanical status of the coil after cool-down, its mechanical properties (elastic modulus and thermal contraction) must be well known.

# Example motivation: Mechanical stored energy generated by $Nb_3Sn$ accelerator magnet heat treatment

# 2. Stress-strain measurements devices
# Capacitive gauges

- The basic principle is to measure the variation of capacity induced by a pressure in a capacitor.
- Being $S$ the area of the two parallel electrodes, $\delta$ the thickness of the dielectric, and $\varepsilon$ the electric permittivity, the capacity $C$ is given by

$$C = \varepsilon S / \delta$$

- When a pressure is applied, the capacity will change

$$C = \varepsilon S / \left[ \delta \left( 1 - \frac{\sigma}{E} \right) \right]$$

- Calibration: the capacity can be measured as a function of pressure and temperature.

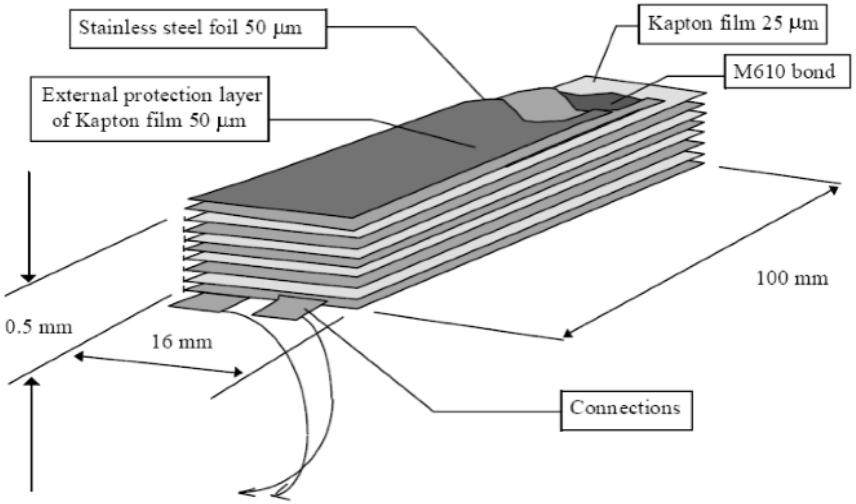


N. Siegel, *et al.*, [1]

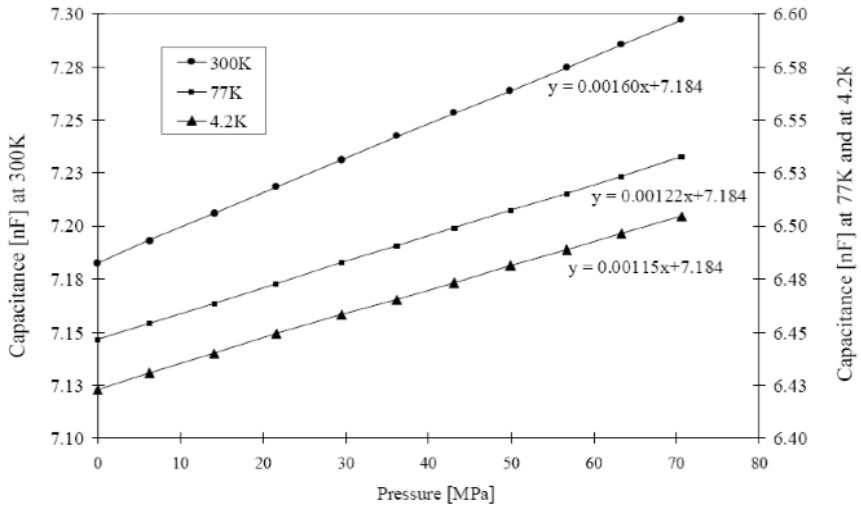


Measurements of strain, stress, and coil

# 2. Stress-strain measurements devices
# Capacitive gauges

- Capacity transducers are typically 0.5 mm thick.
- They can be inserted in between coil and collars in the pole region, or at the coil mid-plane.
- Stress evolution during magnet operation can be monitored
  - Peak stress during collaring
  - Cool-down effect
  - Pole unloading during excitation

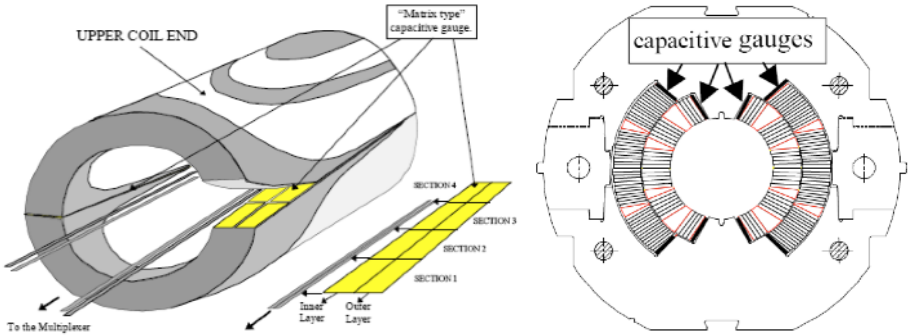


N. Siegel, *et al.*, [1]

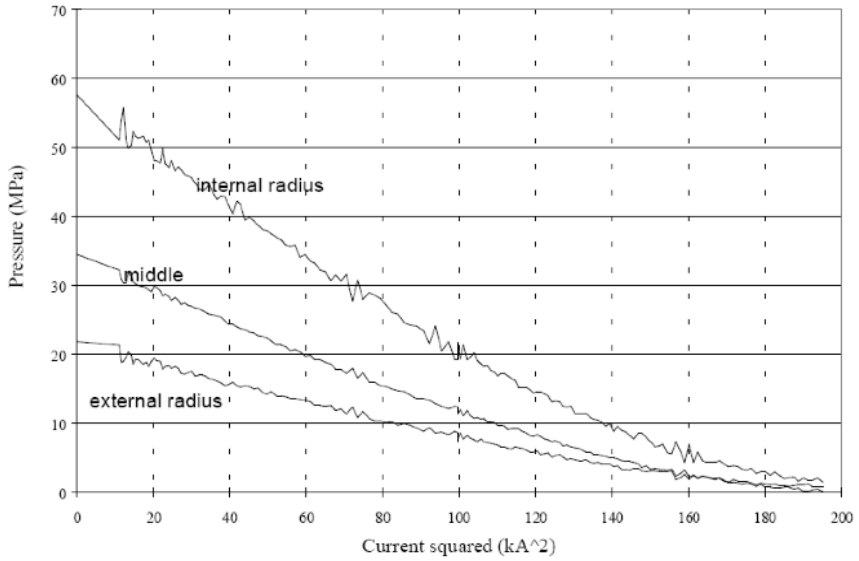

# 2. Stress-strain measurements devices
# Strain gauges

- The basic principle is to measure the variation of resistance induced by a strain in a resistor.
- The gauge consists of a wire arranged in a grid pattern bonded on the surface of the specimen
- The strain experienced by the test specimen is transferred directly to the strain gauge.
- The gauge responds with a linear change in electrical resistance.
- The gauge sensitivity to strain is expressed by the gauge factor

$$GF = \frac{\Delta R / R}{\Delta l / l}$$

- The GF is usually ~ 2.

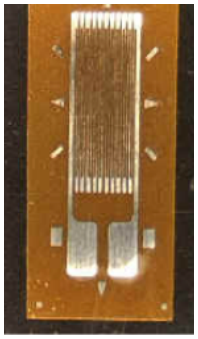

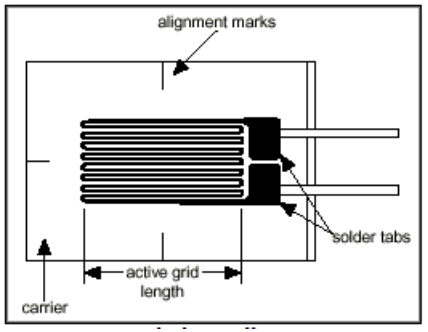


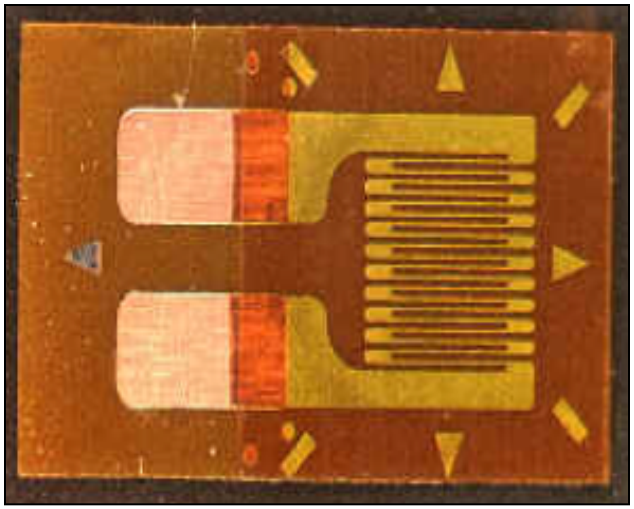

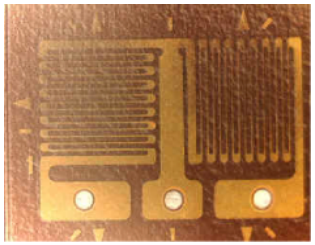

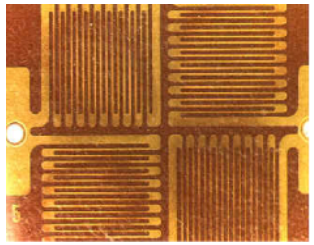

# 2. Stress-strain measurements devices
# Strain gauges

- In case of collar laminations strain gauges can be mounted on beams.
  - The coil stress bends the beam and the gauge measures the strain.
  - Gauges are calibrated by applying a know pressure to a stack of conductors.
- Gauges can also be mounted on solid poles.

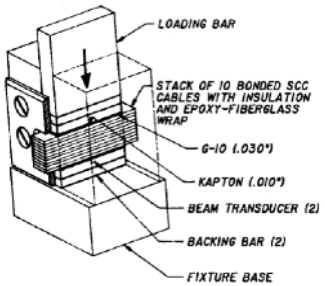


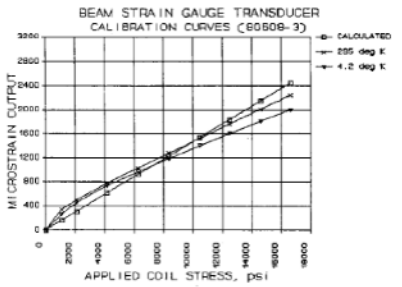


C.L.Goodzeit, *et al.*, [2]

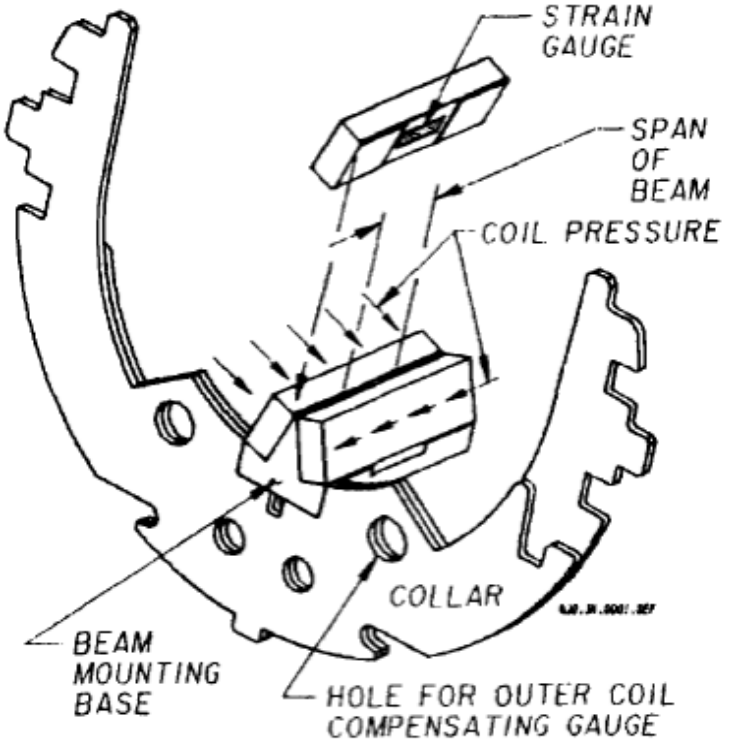


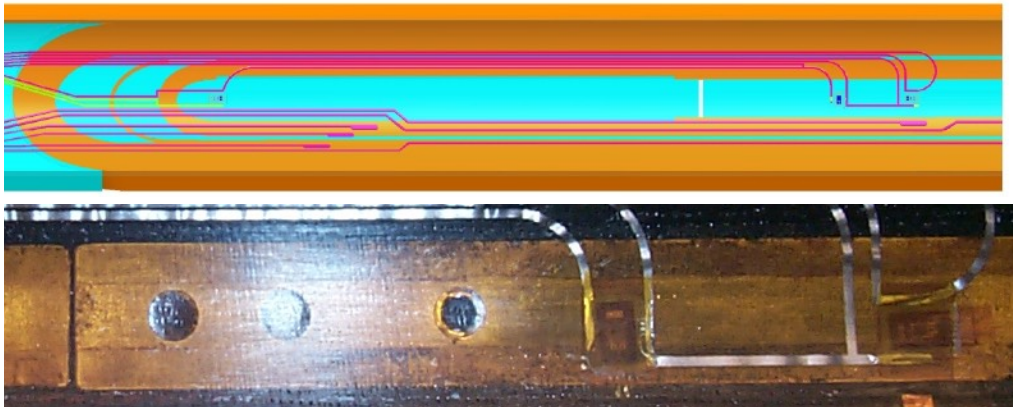

Measurements of strain, stress, and coil

# 2. Stress-strain measurements devices
# Strain gauges

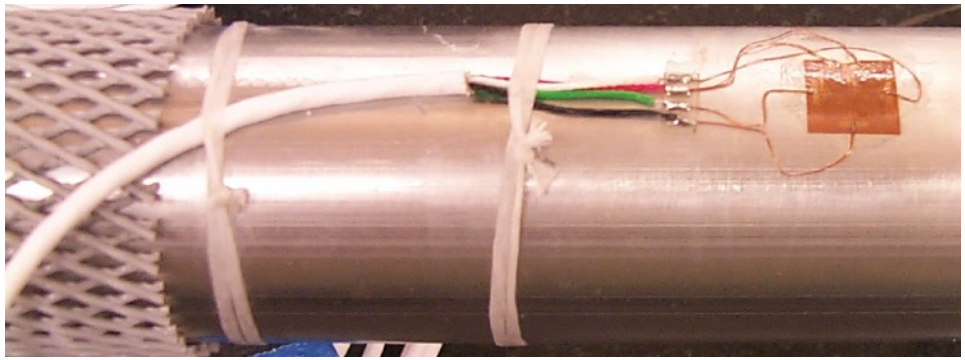

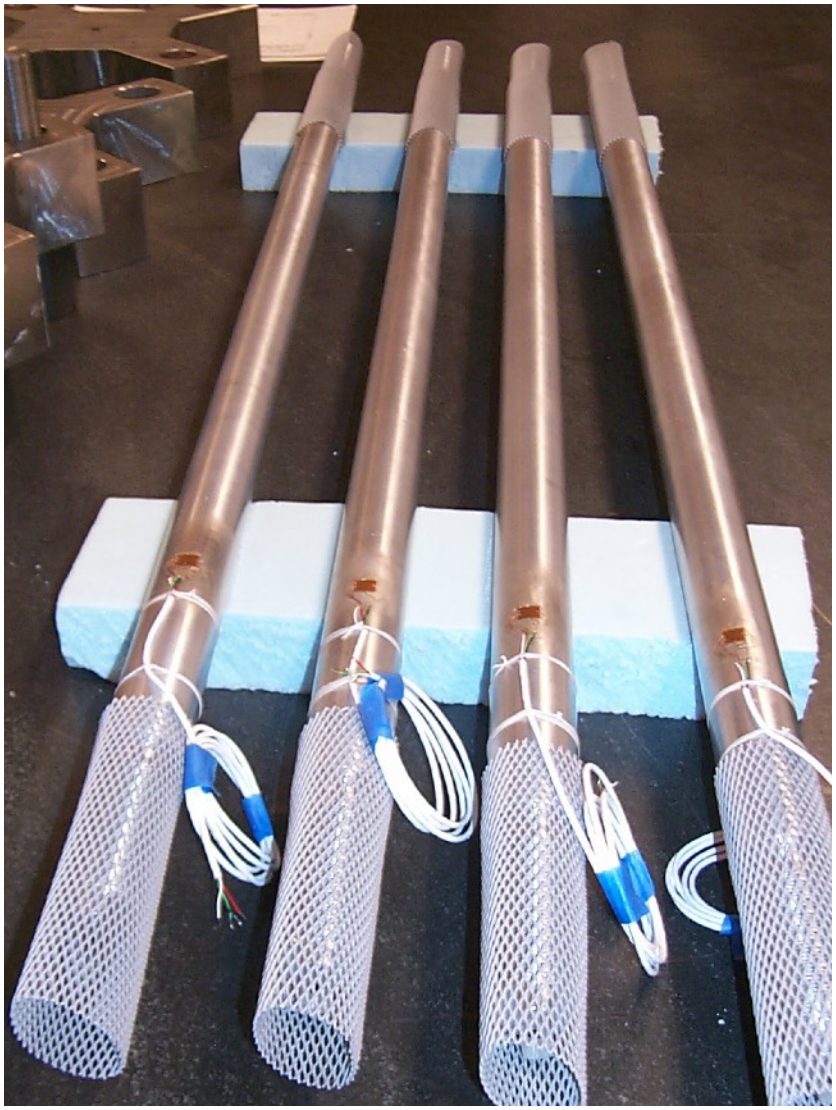

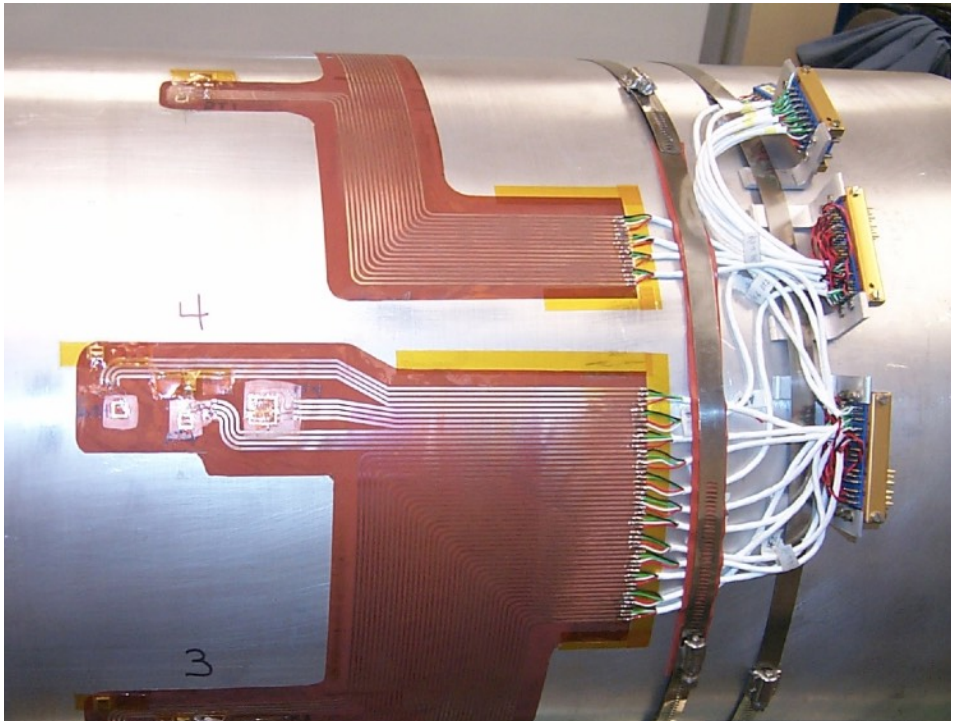


Measurements of strain, stress, and coil

# 3. Measurements of coil properties
# Elastic modulus

- Measurement technique
  - The elastic modulus $E$ is given by

$$E = \frac{d\sigma}{d\varepsilon} = \frac{d\sigma}{dl} l_0$$

  - Where σ is the applied stress, ε the specimen strain, $dl$ the displacement and $l_0$ is the initial length.
  - The measurements procedure consists in compressing a stack of conductors, usually called ten stack, and measuring the induced deformation.

M. Reytier, *et al.*, [3]

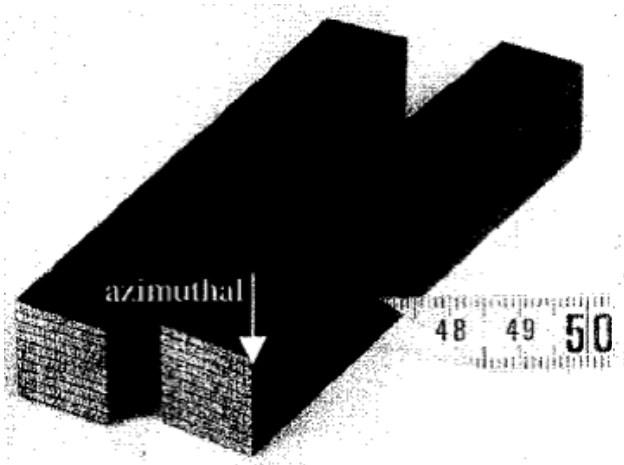


D.R. Chichili, *et al.*, [5]

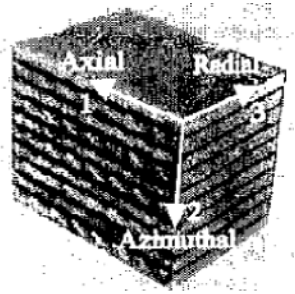


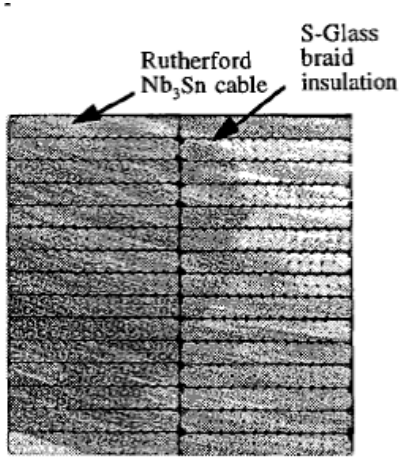


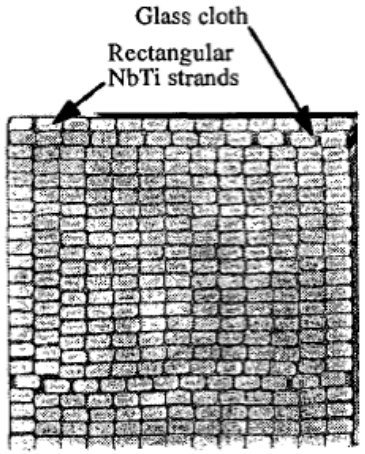


K.P. Chow, *et al.*, [4]

# 3. Measurements of coil properties
# Elastic modulus

- NbTi
  - 293 K
    - The stress-displacement curve is not linear and presents significant difference between loading and unloading phase.
    - The elastic modulus depends on the pressure applied and on the "history" of the loading.

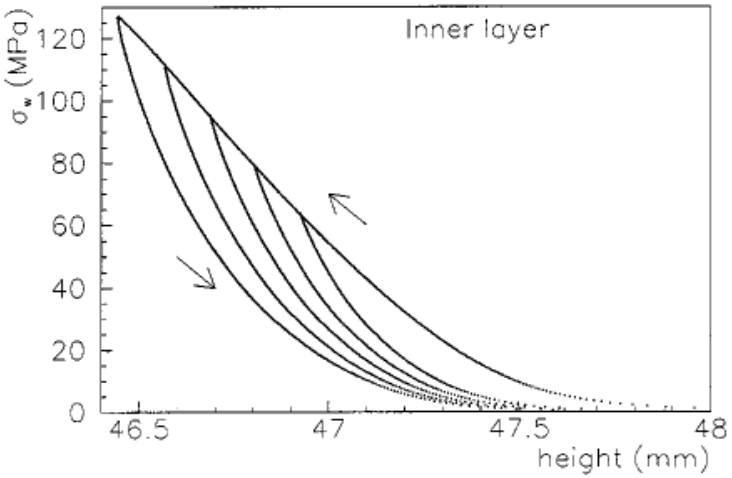


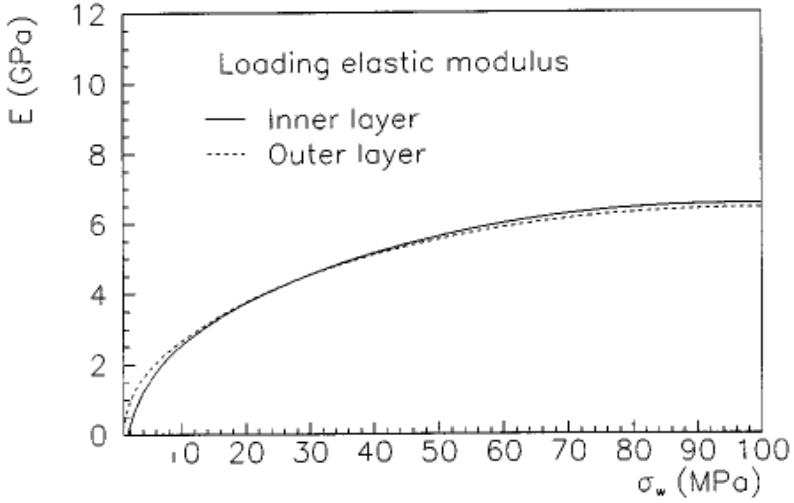


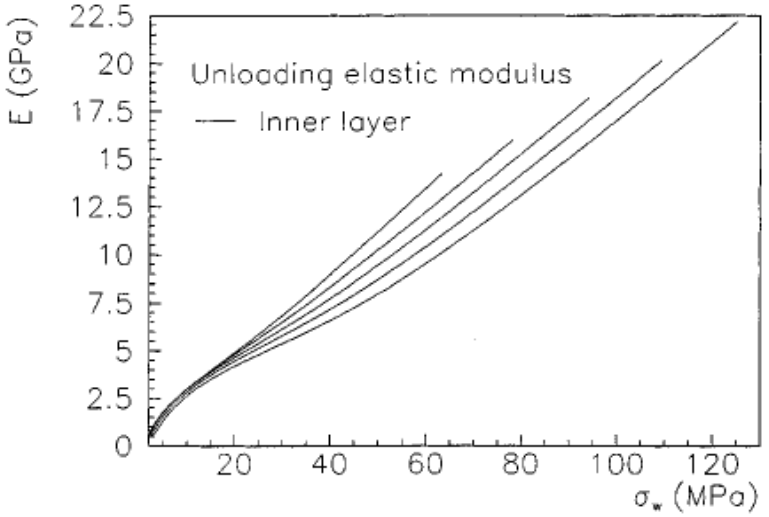


Measurements of strain, stress, and coil

# 3. Measurements of coil properties
# Elastic modulus

- NbTi
  - 77 K
    - The loading branch of the cycle is characterized by steeper slope than at room temperature.
    - The hysteresis between the loading and the unloading curves is considerably smaller.

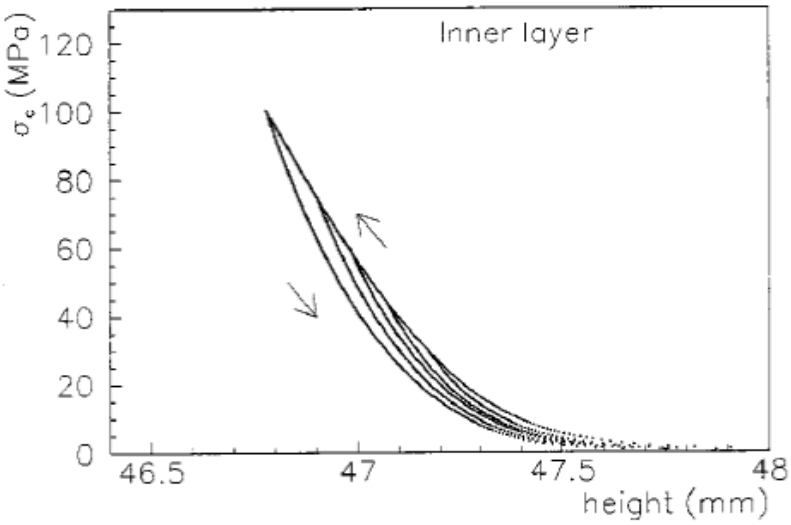


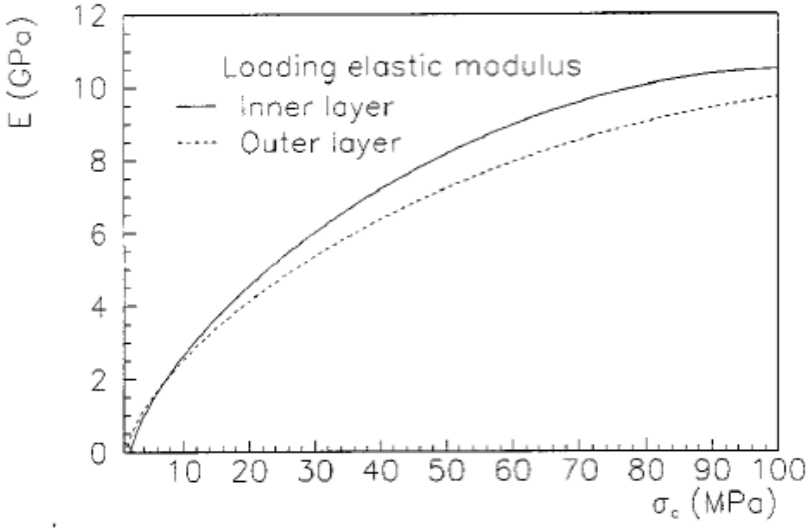


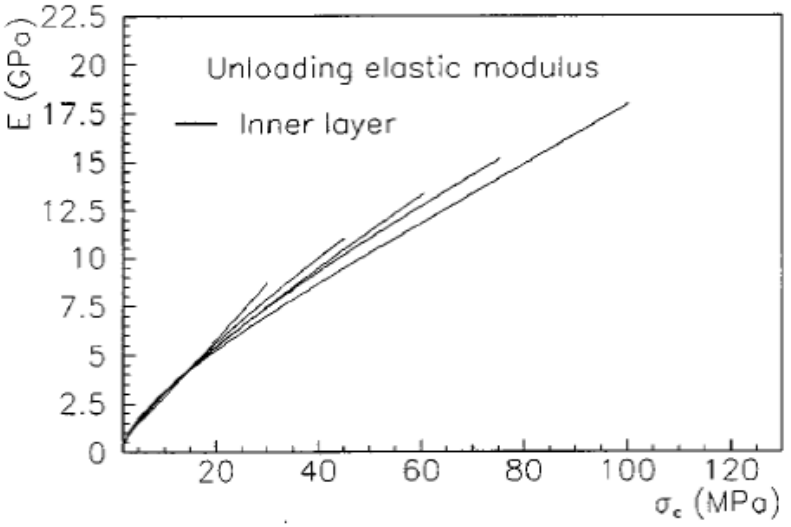


Measurements of strain, stress, and coil

# 3. Measurements of coil properties
# Elastic modulus

- $Nb_3Sn$
  - A similar hysteresis as NbTi cable stack is observed, with an almost linear behavior in the unloading cycles.
  - The modulus, after massaging, is of the order of 35-40 GPa, with no difference between 293 K and 4.2 K.

TABLE III
MECHANICAL PROPERTIES UNDER MONOTONIC LOADING

| Material | $E_{Azimuthal}$, GPa | | $E_{Axial}$, GPa | |
|---|---|---|---|---|
| | 300 K | 4.2 K | 300 K | 4.2 K |
| $Nb_3Sn$ + S-2 Fiber | 18 | 26 | 47 | 56 |
| $Nb_3Sn$ + Ceramic | 27 | 22 | 44 | 55 |

TABLE IV
MECHANICAL PROPERTIES IN AZIMUTHAL DIRECTION AFTER INITIAL LOADING (OR MASSAGING) TO 100 MPa

| Material | E, GPa | | Poisson's Ratio |
|---|---|---|---|
| | 300 K | 4.2 K | |
| $Nb_3Sn$+S-2 | 39 | 40 | $\nu_{12}$= 0.15; $\nu_{32}$= 0.34 |
| $Nb_3Sn$+Ceramic | 38 | 38 | $\nu_{12}$= 0.14; $\nu_{32}$= 0.33 |

D.R. Chichili, *et al.*, [5]

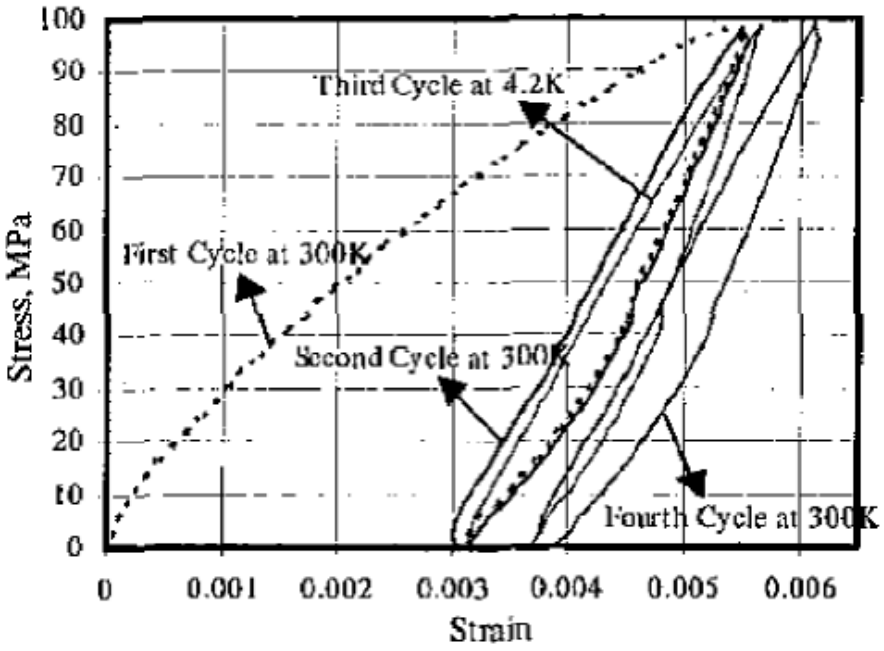


Measurements of strain, stress, and coil

# Nice example of ten-stack measurements

"*Mechanical behavior of MQXF cable stacks at room temperature*", C. Fichera et al.

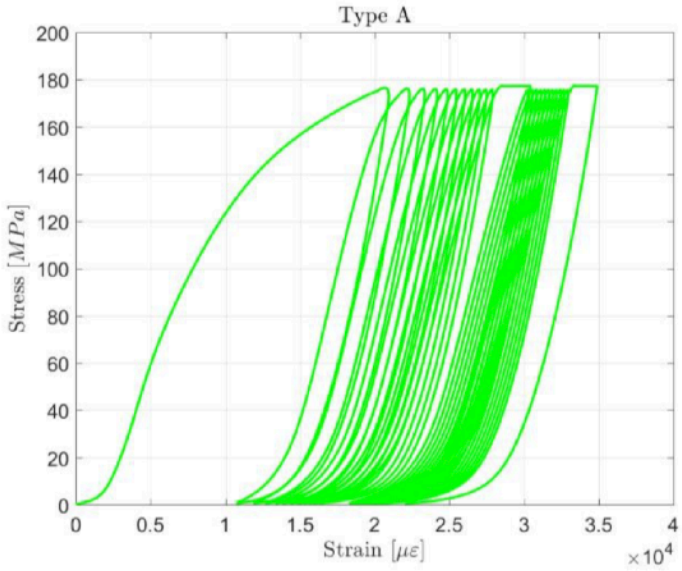


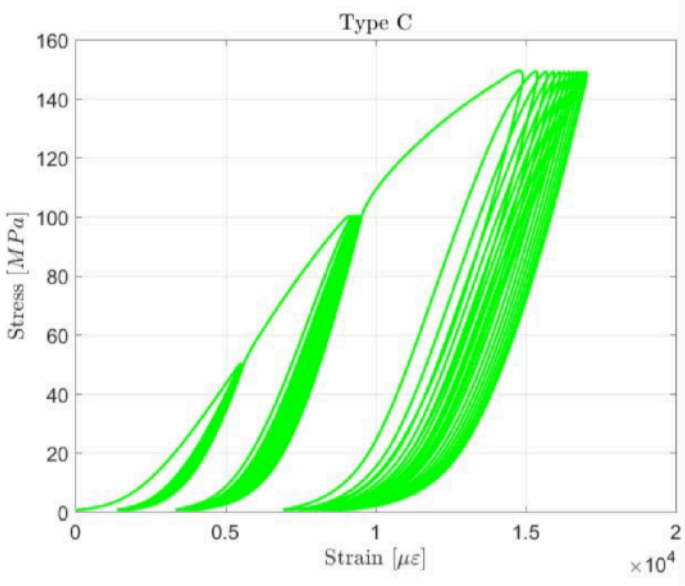


Reaction Mould

Impregnation Mould

Cutting tool

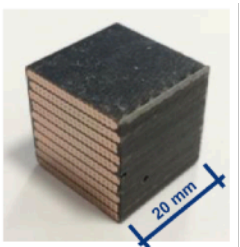


10-Cables stack

# 3. Measurements of coil properties
# Thermal contraction

- Measurement technique
  - The thermal contraction is given by

$$\alpha = \frac{l_{wo} - l_{co}}{l_{wo}}$$

where $l_{w0}$ and $l_{c0}$ are the unloaded height of the specimen respectively at room and cold temperature.

  - It can be also evaluated using the stress loss in a fixed cavity (see Unit 12 Part II). For an infinitely rigid cavity one gets

$$\sigma_{cs} = \frac{E_{cs}}{E_{ws}}\left[\sigma_{ws} - E_{ws}\left(\alpha_f - \alpha_s\right)\right]$$

  - By measuring the stress loss, one obtains $\alpha_s$.

D.R. Chichili, *et al.*, [5]

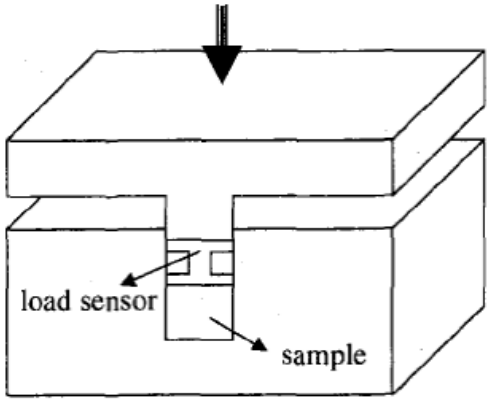


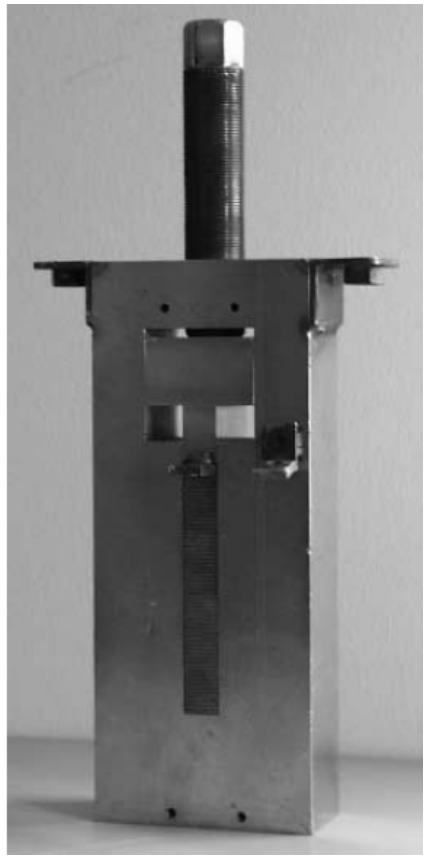

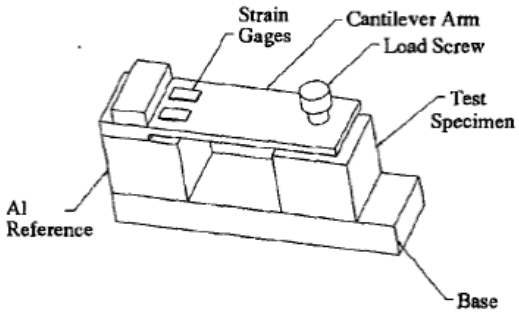


K.P. Chow, *et al.*, [4]

Measurements of strain, stress, and coil

# 3. Measurements of coil properties
# Thermal contraction

- NbTi
  - A strong the dependence of the thermal contraction on the stress applied before the cool-down is observed
    - $6 \times 10^{-3}$– $8 \times 10^{-3}$ for 40-60 MPa
    - $9 \times 10^{-3}$– $12 \times 10^{-3}$ for 70-80 MPa

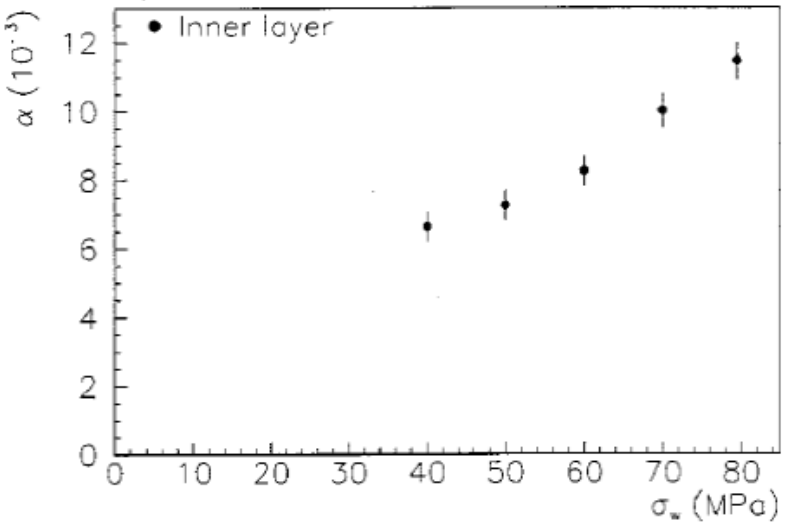


- $Nb_3Sn$
  - Data available in literature indicate a thermal contraction ranging from $3.3 \times 10^{-3}$ to $3.9 \times 10^{-3}$.

TABLE IV
INTEGRATED THERMAL SHRINKAGE COEFFICIENT BETWEEN 293 K AND 4.2 K

| Sample | Number of Tests | Test Result (mm/m) | Literature (mm/m) |
|---|---|---|---|
| Copper | 1 | –3.4 | –3.24 [7] |
| S. Steel | 1 | –2.9 | –3.06 [7] |
| Resin | 2 | –18.8 ±0.1 | –11.6 [7]<br>up to –14 [12] |
| $Nb_3Sn$ Stacks | 2 | –3.9 ±0.1 | –3.50 [9]<br>–3.30 [8] |
| Impregnated NbTi Stacks | 2 | –3.8 ±0.1 | –3.55 [8] |
| NbTi + Kapton Stacks | | –4.96 [2] | |

D.R. Chichili, *et al.*, [5]

# Experience with HQ demonstrated that proper confinement dimensioning is critical

From H. Felice, "Status on HQ Coil Design and Fabrication", 17th LARP, 1st HiLumi collaboration meeting

**Study on unconfined cables**

Meas. performed at LBNL by J. Krishnan

- axial contraction: 0.1 to 0.3 %
- thickness increase: 1.4 to 4 %
- width increase: 1.5 to 2 %

**Study on sections of LQ - TQ and HQ coils**

**Thickness**
LQ and TQ: 5.6 and 6% of increase
HQ: only 1 to 2 % of increase

**Width**
LQ and TQ => 1 to 2 % of increase
HQ => 1 % of increase

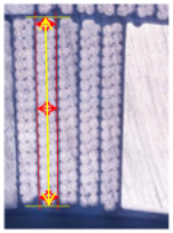

Meas. Performed at FNAL D. Bocian, M. Bossert


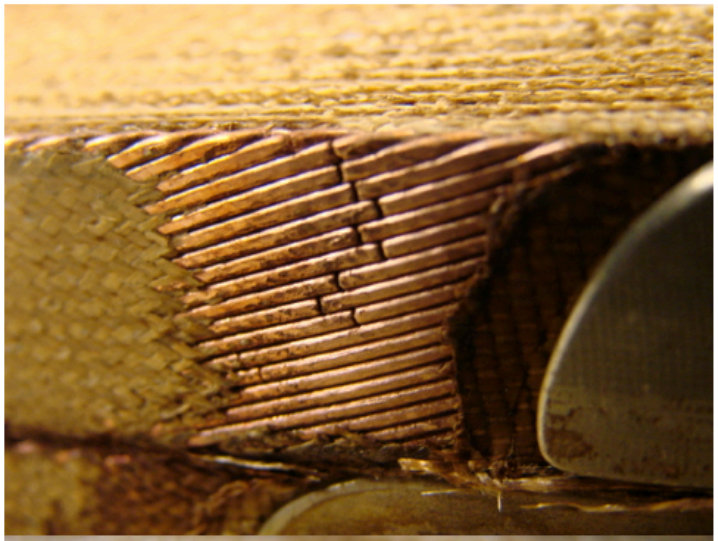

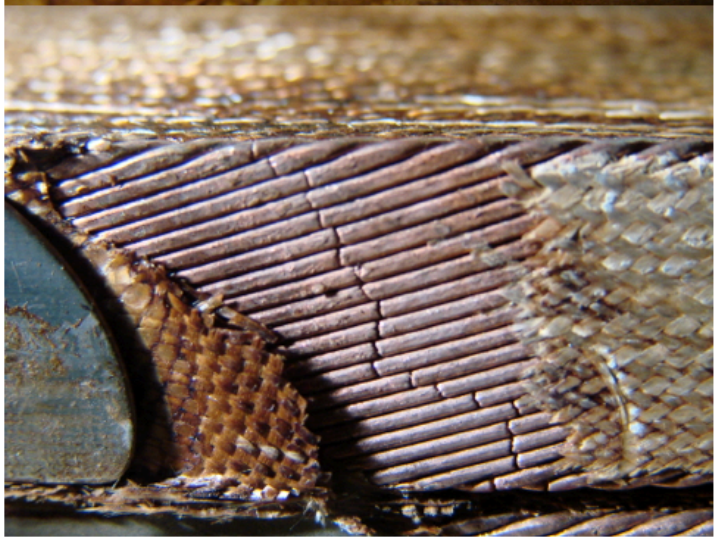

Solution in HQ case was to provide more "room" for cable expansion during reaction

# Early work looked at what phase of the heat treatment is the source of length change

**DIMENSIONAL CHANGES OF $Nb_3Sn$, $Nb_3Al$ AND $Bi_2Sr_2CaCu_2O_8$ CONDUCTORS DURING HEAT TREATMENT AND THEIR IMPLICATION FOR COIL DESIGN**

ICMC '97

D.R. Dietderich, J.R. Litty, and R.M. Scanlan

Lawrence Berkeley National Laboratory
Berkeley, CA, 94720, U. S. A.

Change in dL/dT due to different volume fraction after formation of intermetallics

Expansions with composite nature; Nb and Cu mix. Length increases with temperature similar to Cu

Formation of Cu-Sn phases results in density change – no increase in length, or even contraction

Conductor elongates with temperature

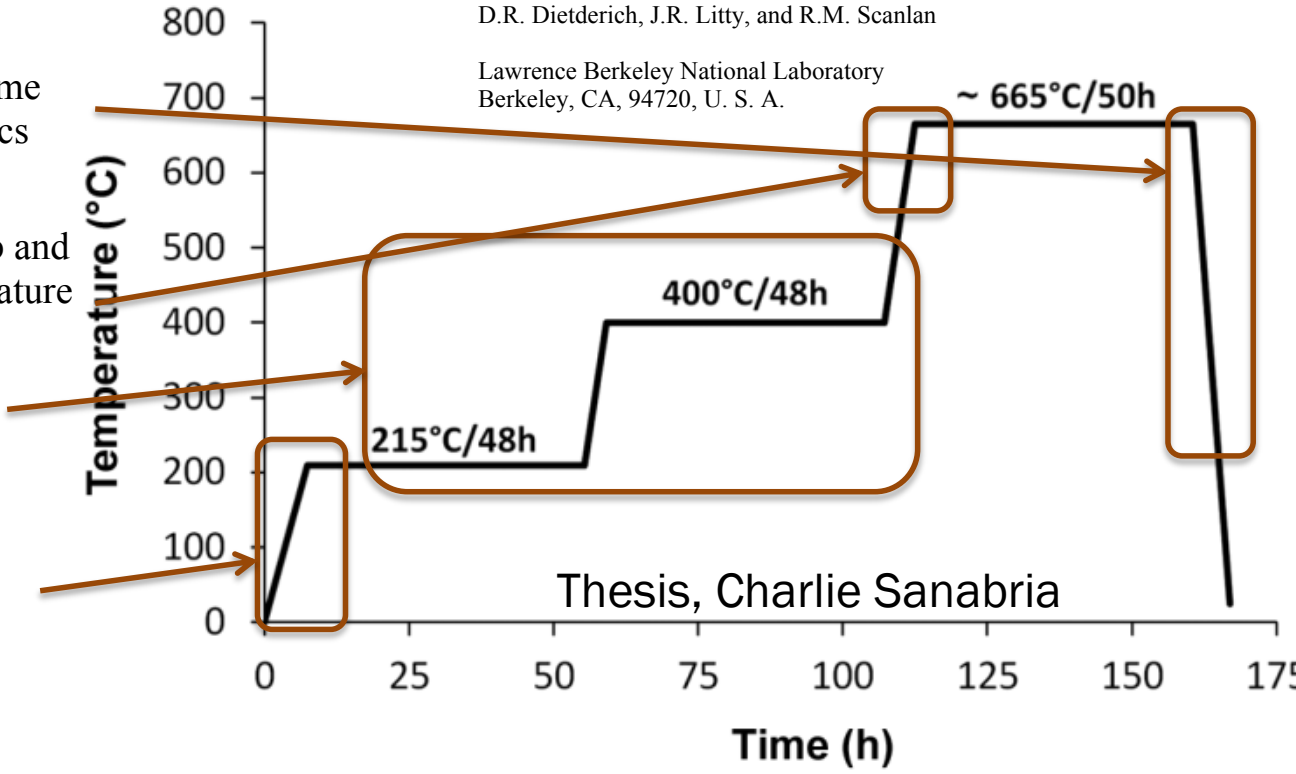


Figure 42 The standard heat treatment for RRP® wires since 2005.

# Early dilatometry measurements provide some insight into mechanics of wires during reaction

*Notes:*
*- this is not a full reaction cycle for the $Nb_3Sn$ wire (faster ramp, no holds, etc)*
*- 19 sub-element IGC-AS Internal-tin wire*

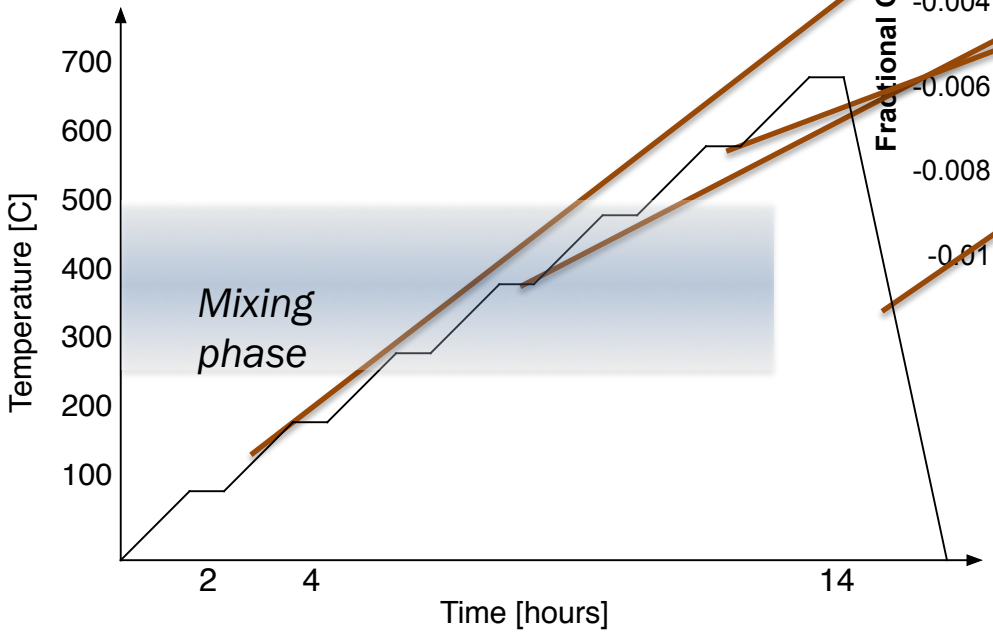


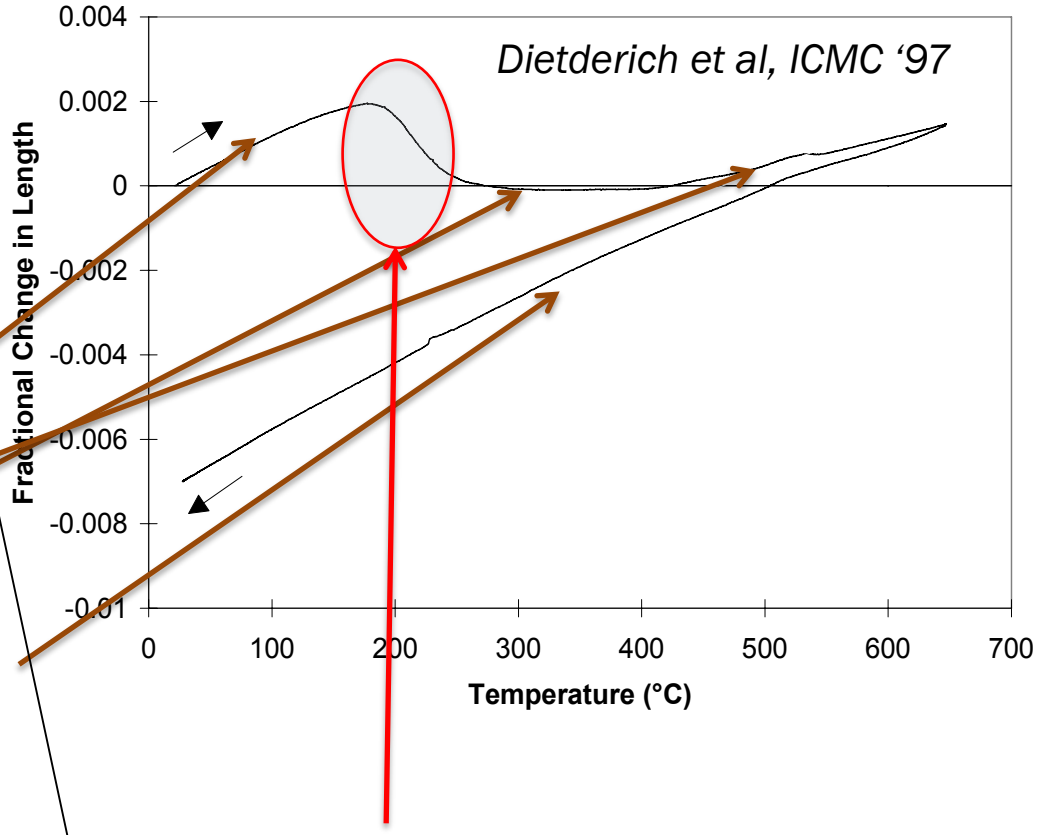


What is the source of the "dip"?

# Conclusions are…

No annealing ⇒ residual stress

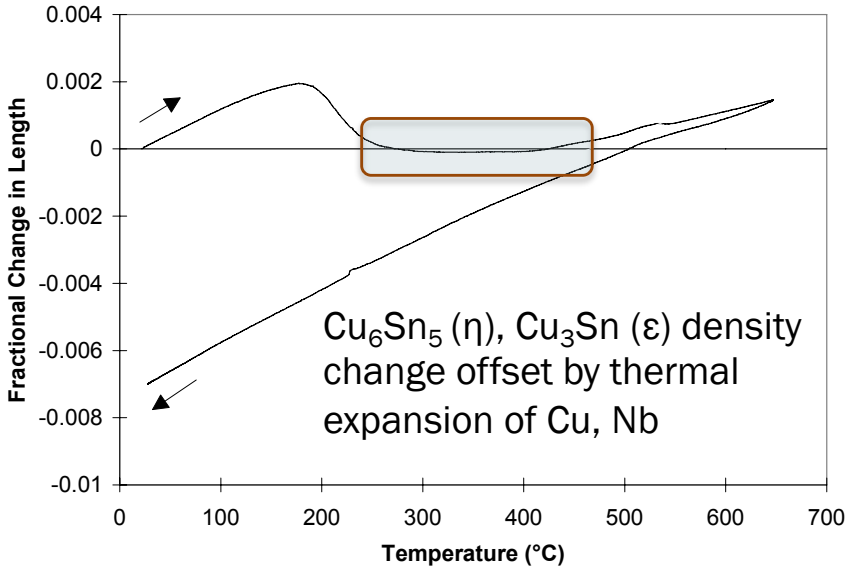


(a)

Annealed during processing
⇒No residual stress

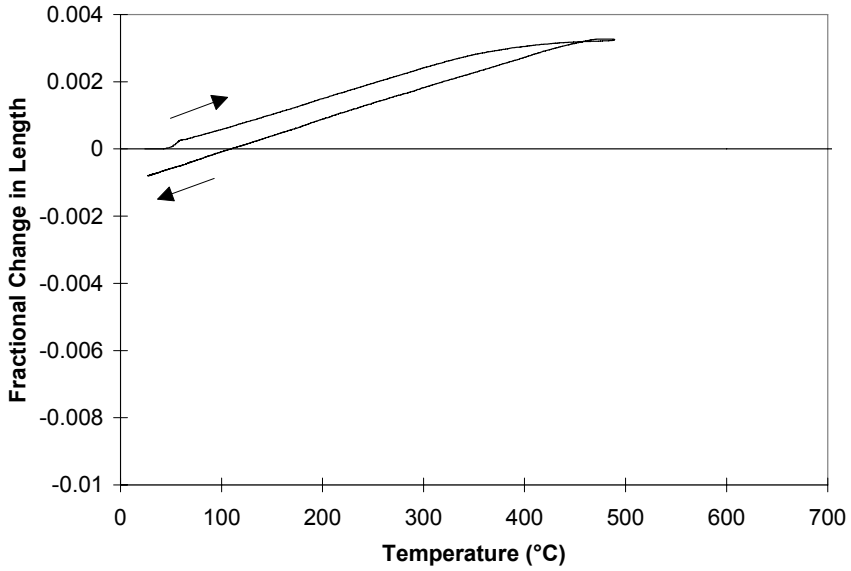


(b)

Figure 3. (a) Fractional change in length of an ITER conductor produced by IGC-AS. This 19 sub-element wire with 50 % Cu is the same conductor as seen in figure 1(b). (b) Fractional change in length of a bronze-processed conductor produced by Hitachi. Same as the conductor of figure 1(a).

**Conclusion**: dip at 210C is due to stress relief between Nb tension and Cu, not Cu-Sn intermetallic phase creation

**Note:** these measurements do not tell us about the radial growth vs T

# Systematic studies on LARP cables show some interesting correlations

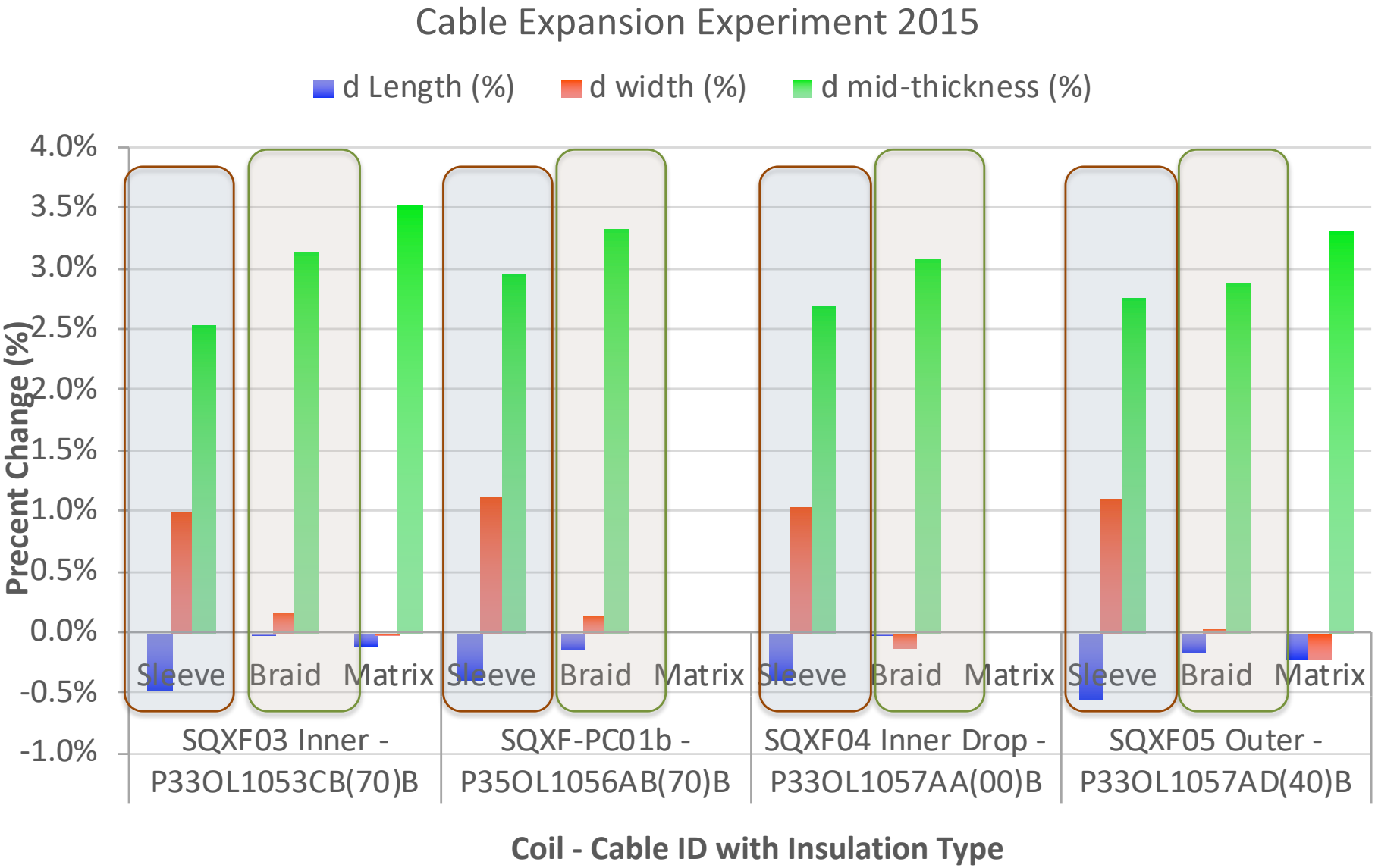

# Some conclusions

- Confined and unconfined cables behave differently
  - Width and thickness always increase; length shrinks when unconfined whereas cable elongates when confined
  - Volume is not fully conserved; void formation varies
- Braid and sleeve have different effect on cable dimension change during heat treatment → impact of insulation
  - braid is like a cable with width confined
- "Matrix material" degrades the braid but the effect on cable dimension change is similar: ~3% increase in mid-thickness

# Hierarchical modeling to obtain stress states

- The idea of modeling the many scales associated with accelerator magnets has lead to some significant progress, but we have

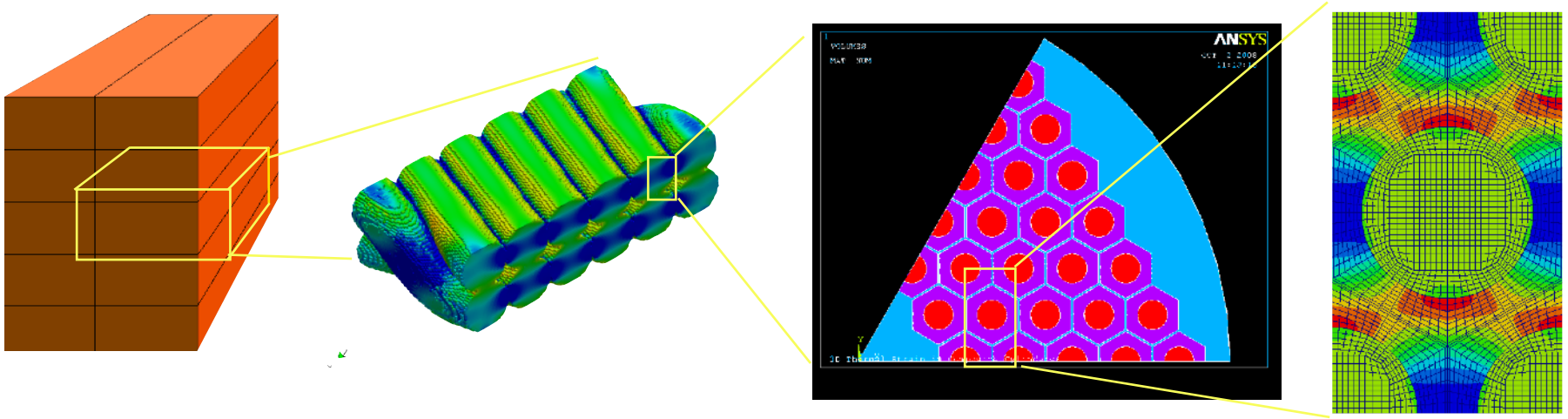


D. Arbelaez, S. O. Prestemon, P. Ferracin, A. Godeke, D. Dietderich, and G. Sabbi, "Cable Deformation Simulation and a Hierarchical Framework for Nb3Sn Rutherford Cables," EUCAS, pp. 1–11, Sep. 2009.

# An example of modeling the deformations associated with cabling

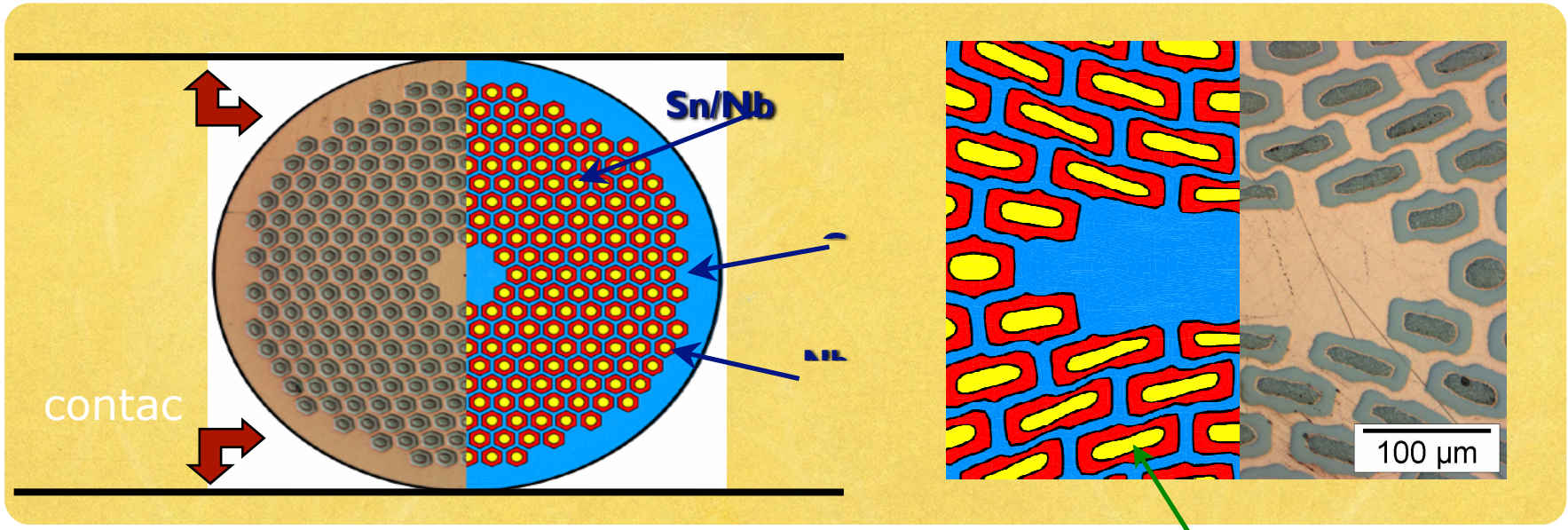


*S. Farinon, Presented at CHATS-AS 2006*

Access to 2D strain tensor!
(Simulated)

# Modeling macroscopic strand deformations as a step towards modeling cables in coils

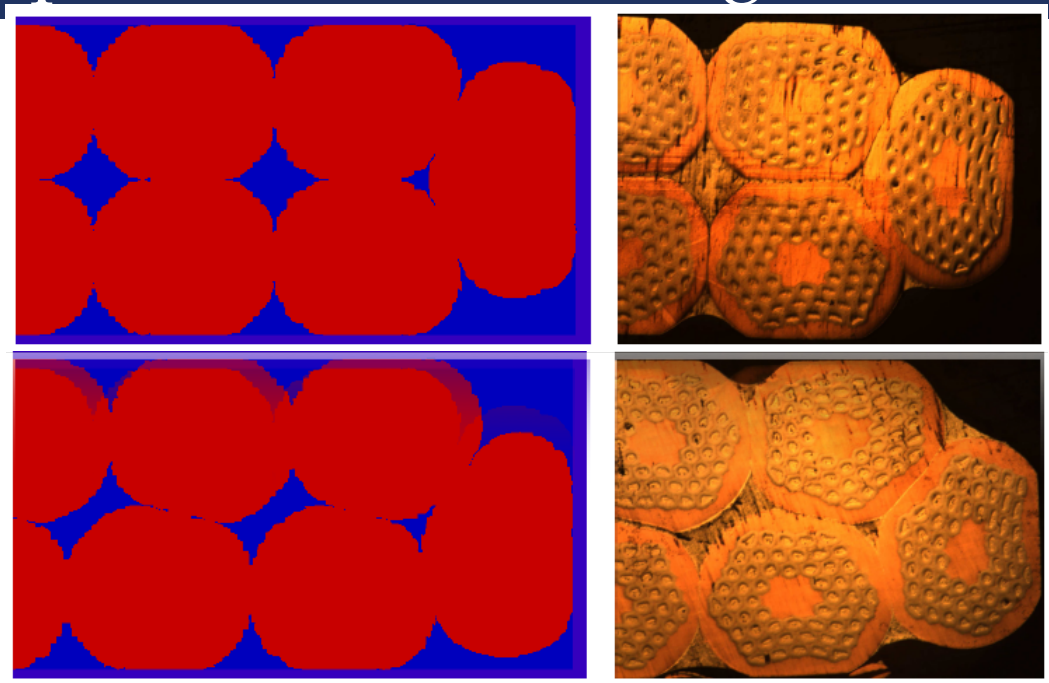

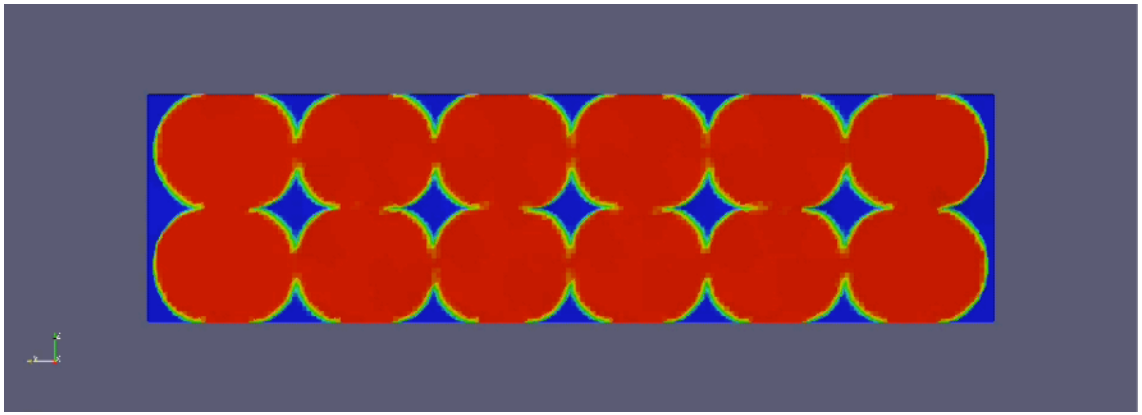

# Homogenization of the "Coil Material"

- ★ "Coil Material" microstructure
  - ✓ Cable
  - ✓ Interstitial binder (epoxy)
  - ✓ Insulation layer (S-glass composite)
- ★ Homogenized strand properties are used for the cable
- ★ Periodicity is assumed in all directions (infinite material)
- ★ Consider only linear elastic behavior
- ★ Effective properties are extracted by applying six different periodic loading conditions

$$\langle \boldsymbol{\sigma} \rangle_\Omega = \mathbb{E}^* : (\langle \boldsymbol{\epsilon} \rangle_\Omega - \boldsymbol{\alpha}^* \Delta\theta)$$

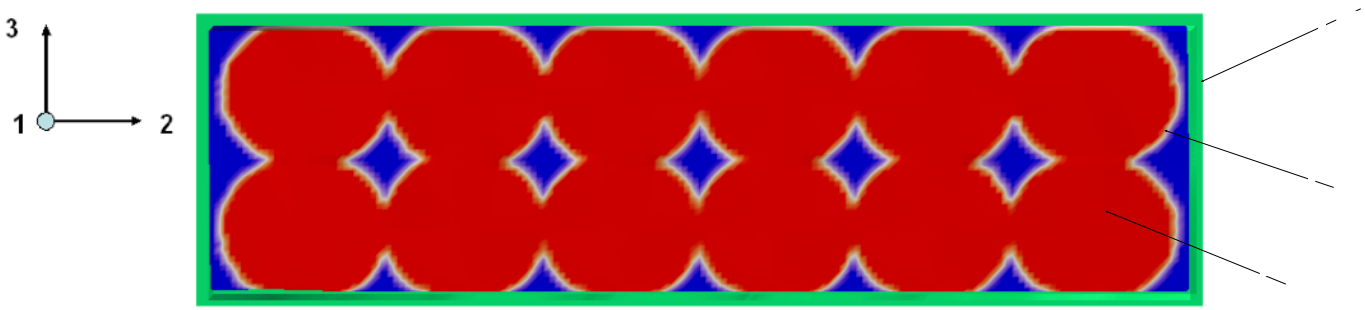

# Model at the Strand/Filament Scale

- Homogenization of a periodic microstructure to determine effective properties
  - Periodic assumption is valid only if there is a large number of sub-elements
  - Geometry may not be periodic due to deformations
- Plasticity is included in the model but not yet in the coupling framework

$$\langle \boldsymbol{\sigma} \rangle_\Omega = \mathbb{E}^* : (\langle \boldsymbol{\epsilon} \rangle_\Omega - \boldsymbol{\alpha}^* \Delta\theta)$$

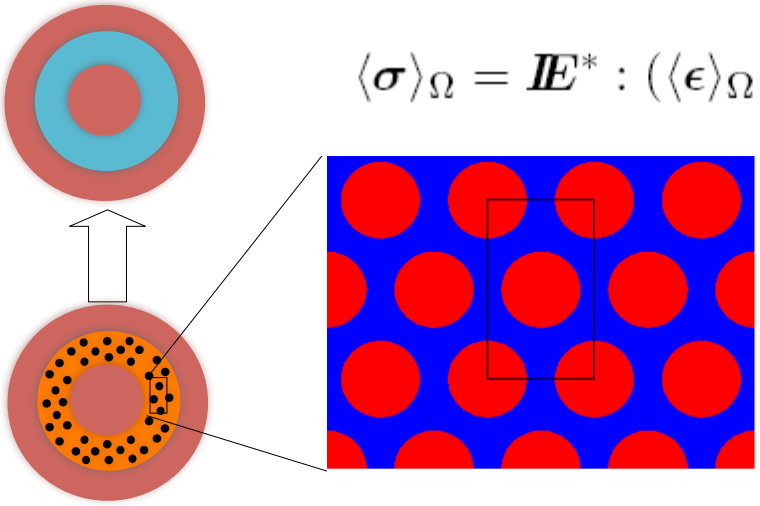

Periodic Microstructure

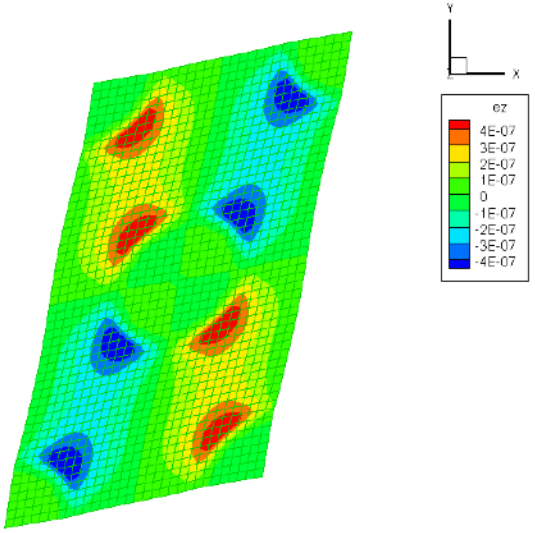


Periodic Boundary Conditions

# Coupling Between Different Scales

- ★ Currently the coupling is for only linear elastic properties
  - ✓ Trivial coupling between scales since properties are independent of deformation
  - ✓ Coupling from coil to cable scale and from cable to RRP sub-element/filament scale
- ★ Loads are transferred by applying the strain in the larger scale as the average strain over a unit cell in the smaller scale

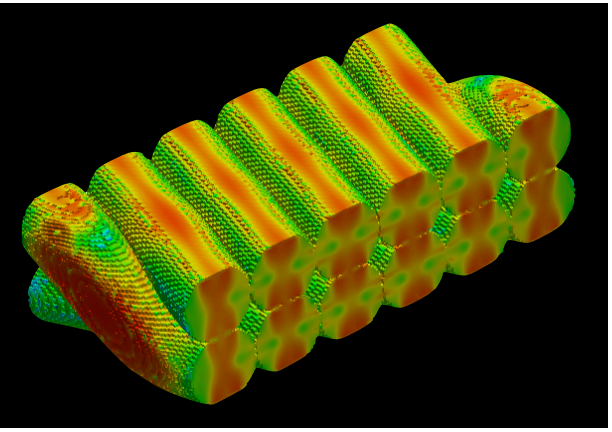

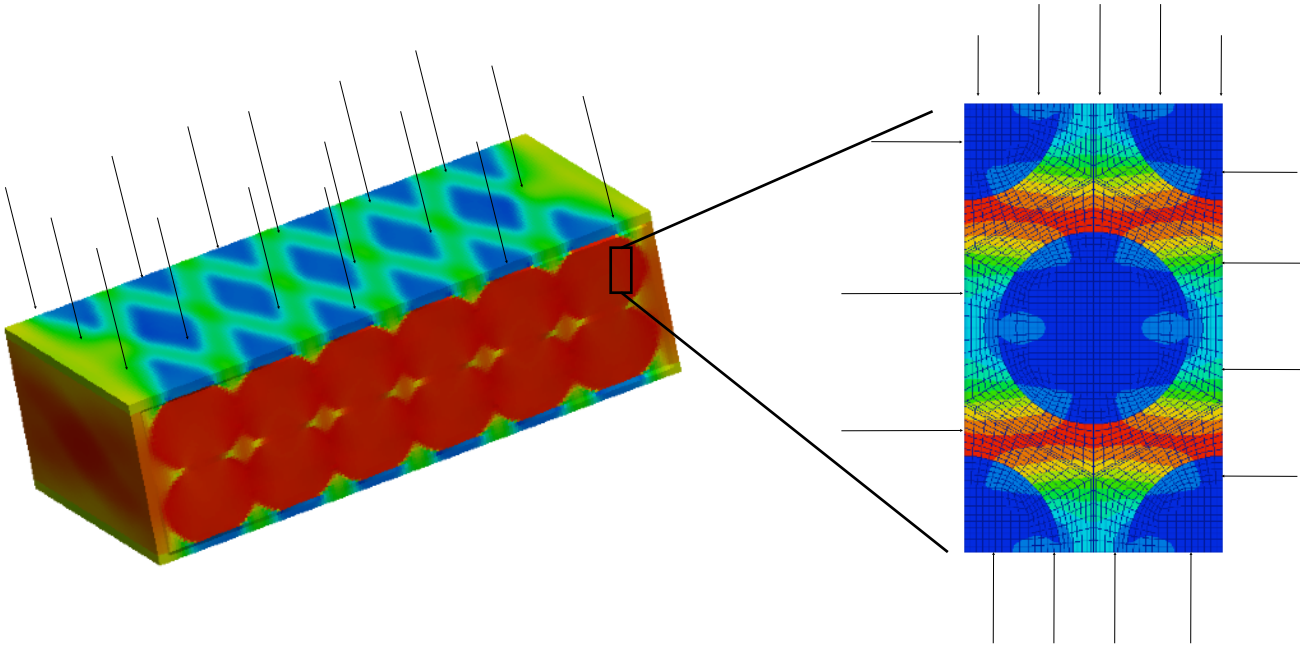

# Example: Calculated Orthotropic "Coil Material" Properties

- Individual Material Properties
  - Epoxy (E = 5 GPa, ν = 0.3)
  - Insulation ($E_l$ = 14.9 GPa, $E_t$ = 6.7 GPa)
  - Strand properties varied (E = 126 GPa determined from homogenization of the strand with E = 135 GPa for $Nb_3Sn$)
  - These properties are estimates, there is need for accurate measurements

$E_s$: Apparent strand Young's modulus
$E_i$: Young's modulus in i direction
$\nu_{ij}$: Poisson's ratios
$\mu_{ij}$: Shear moduli

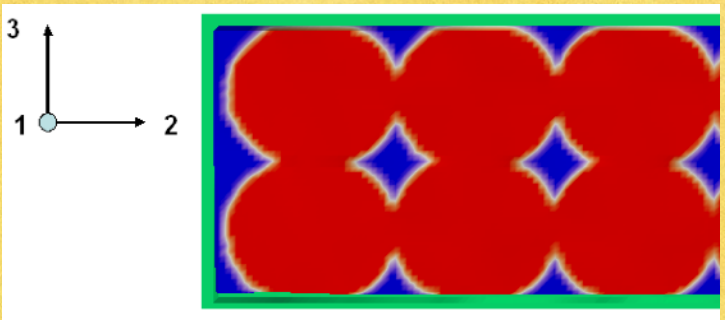


| | 100 $\mu m$ insulation | | | 60 $\mu m$ insulation | | |
|---|---|---|---|---|---|---|
| $E_s$ (GPa) | 90 | 110 | 126 | 90 | 110 | 126 |
| $E_1$ (GPa) | 65.1 | 78.7 | 89.5 | 68.5 | 82.8 | 94.5 |
| $E_2$ (GPa) | 41.0 | 45.8 | 49.3 | 45.7 | 51.7 | 56.1 |
| $E_3$ (GPa) | 27.8 | 29.7 | 30.9 | 34.0 | 36.8 | 38.8 |
| $\nu_{12}$ | 0.34 | 0.34 | 0.34 | 0.34 | 0.34 | 0.34 |
| $\nu_{23}$ | 0.24 | 0.23 | 0.22 | 0.25 | 0.24 | 0.23 |
| $\nu_{31}$ | 0.14 | 0.12 | 0.11 | 0.16 | 0.14 | 0.13 |
| $\mu_{12}$ (GPa) | 19.4 | 22.0 | 23.8 | 20.5 | 23.5 | 25.7 |
| $\mu_{23}$ (GPa) | 13.7 | 14.9 | 15.6 | 15.2 | 16.8 | 17.8 |
| $\mu_{31}$ (GPa) | 14.8 | 16.1 | 17.0 | 16.8 | 18.8 | 20.2 |